Pilot *Ex Vivo* Study of Laser-Induced Breakdown Spectroscopy to Detect Bone Dehydration: An Approach for Irrigation Feedback in Laserosteotomy

Hamed Abbasi
Biomedical Laser and Optics Group, Department of Biomedical Engineering
University of Basel
Allschwil, Switzerland
hamed.abbasi@unibas.ch

Raphael Guzman
Department of Neurosurgery
University Hospital Basel
Basel, Switzerland
raphael.guzman@unibas.ch

Irena Sugiarto
Department of Biomedical Engineering
Swiss German University, Tangerang, Indonesia, *and*
University of Basel
Allschwil, Switzerland
irena.sugiarto@student.sgu.ac.id

Philippe C. Cattin
Center for medical Image Analysis and Navigation, Department of Biomedical Engineering,
University of Basel
Allschwil, Switzerland
philippe.cattin@unibas.ch

Georg Rauter
Bio-Inspired RObots for MEDicine-Lab, Department of Biomedical Engineering,
University of Basel
Allschwil, Switzerland
georg.rauter@unibas.ch

Azhar Zam
Biomedical Laser and Optics Group, Department of Biomedical Engineering
University of Basel
Allschwil, Switzerland
azhar.zam@unibas.ch

***Abstract*— A successful laserosteotome should cut the bone without inducing thermal damage to the surrounding tissue, otherwise the healing process will be prolonged. To avoid such thermal damage, laserosteotomes typically employ an irrigation system with a pre-defined flow rate of cooling water. If this pre-defined flow rate is insufficient, for any reason, the laser beam will induce thermal damage by first dehydrating and then carbonizing the tissue. On the other hand, a too high water flow rate will result in lower ablation rates since the laser beam first needs to ablate the extra water before cutting bone, especially with lasers that water has a high absorption peak in their wavelengths, like Er:YAG and CO_2. While a feedback mechanism detecting carbonization has been demonstrated in literature already, it would be desirable to detect possible dehydration at an earlier stage (underirrigation) where the tissue damage is still negligible. This pilot study evaluates the applicability of laser-induced breakdown spectroscopy (LIBS) to detect bone dehydration already at its onset. The results confirmed a good accuracy of over 89 % (cross-validated) in classifying normal and dehydrated bone.**

Keywords*— LIBS, plasma spectroscopy, bone dehydration, minimally invasive surgery, laserosteotome

I. INTRODUCTION

In order to replace conventional bone cutting tools with laserosteotomes, laser systems have to cut the bone in a fast and safe manner without inducing any thermal damage to the surrounding tissue. Therefore, the beam of the laser needs to be complemented with an irrigation system to avoid thermal damage [1-6]. The flow rate of the water in the irrigation system should be set optimally as too little water causes carbonization of the bone or too much water reduces the cutting speed and achievable maximum cutting depth [7, 8]. Without any irrigation, the bone dehydrates after only a few laser pulses and then starts to carbonize [7, 8]. A feedback mechanism on dehydration would thus be suitable to control the flow rate of the irrigation system. Laser-induced breakdown spectroscopy (LIBS) has been reported to be a fast and accurate analytical technique for detecting the type and properties of the tissues [9-20]; therefore, this method looks as a promising candidate to detect dehydration as well. Moreover, the authors have shown that laser-induced bone carbonization is detectable through a LIBS-based feedback mechanism [21]. Feedback on carbonization could help to stop further carbonization in laserosteotomy, while successful feedback on dehydration could help preventing carbonization in the first place, as dehydration is the precursory stage of carbonization. This pilot study examines the applicability of LIBS to discriminate fresh from dehydrated bone. A porcine femur bone bought from a local slaughterhouse (kept in the freezer before the experiment), was used as the non-dehydrated sample, henceforth called "fresh sample". Also, a bone which was left open under room temperature conditions for 10 days was used as a "dehydrated sample". We assumed that crystallization of water content of the bone in the freezer has not any significant effect on our result. A total of 50 laser shots from each sample were measured. Assuming that the dehydration caused by gradual evaporation on the dehydrated bone happens in a similar fashion to laser-induced dehydration and there is no major chemical decomposition over these 10 days, this detection approach could be transferred to the real-time feedback system of laserosteotomes.

Funded by Werner Siemens Foundation through the MIRACLE project.

II. MATERIALS AND METHODS

A. Bone Preparation

Two bisected porcine femur bone samples were used in this study. One bone was kept in room temperature for ten days, after removing the surrounding soft tissues (the dehydrated sample). The other bone sample was kept in a freezer to keep the water content stable (the fresh sample). The freezer temperature was set to − 18° C. Four hours prior to the experiment the specimen was moved from the freezer

to the refrigerator with a temperature of +4° C. Later on, the surrounding soft tissues were removed from the surface of the bone with the help of a surgical scalpel. The experiments were carried out at room temperature.

B. Ethics Committee Approval

Since the used bone samples were commercially available as regular food obtained from the local slaughterhouse, ethics committee approval was not necessary.

C. Laser Source

The second harmonic beam line of a flashlamp-pumped Q-switched Nd:YAG laser (Q-smart 450, Quantel, France) at 532 nm was used to perform plasma-mediated ablation in both groups of samples. The laser emitted a pulsed beam with a duration of 5.2 ns and linewidth (FWHM) of fewer than 0.7 cm^{-1}. The energy and repetition rate of the laser were set to 108 mJ and 1 Hz, respectively. More information about the generation, separation, and blocking of the harmonics of the laser setup is explained in our previous work [11, 21]. The frequency-doubled output beam of the laser with 6.5 mm diameter was horizontally directed to an uncoated Calcium Fluoride plano-convex lens (LA5458, Thorlabs, USA) with a focal length of 80 mm which was placed perpendicular to the laser line and optical table. The high focusability of the employed laser (M-squared of less than 2), provided a high power density at the focal point. The focused light was guided to the surface of the bone samples from the side to generate a microplasma at the surface of the specimens.

D. Spectroscopy Setup

Due to the need for both, a high power resolution combined with a large bandwidth, an Echelle spectrometer was chosen to be used in this study for analyzing the emitted light from the laser-induced microplasma. The employed Echelle spectrometer resolved the input light with the resolving power of better than 4000 [a.u.] in the interval of 200 to 975 nm (aperture F/7). In total, the input light was separated into more than 28000 different wavelengths. A 16-bit intensified CCD (ICCD) with a built-in delay generator was used as the detector of the spectrometer. The spectrometer was synchronized with the Q-switch of the laser using a TTL 5 pulse to apply the desired time delay (Q-switch as a master and the spectrometer as a slave). The gate delay of 5 µs was applied to avoid collecting continuum radiation which could hide the atomic and molecular lines of the generated microplasma [22, 23]. In order to increase the signal to noise ratio (SNR), the ICCD was cooled down to − 30° C to minimize the background noise (during the calibration and also the experiment). The experiments were run at the same temperature that was employed during calibration of the spectrometer (+ 25° C) in order to avoid misalignment caused by thermal expansion/contraction of the system. A UV–NIR light collector with an F-number of 2 connected to a fiber optic with a 50 µm core was used to collect the plasma emission light and deliver it to the spectrometer. No polarization/spatial-resolved technique was employed. All spectra were recorded in a time-resolved manner. Figure 1 shows the schematic of the employed time-resolved LIBS setup. As has been shown in the figure the plasma light was collected at 45° in reference to the incident beam.

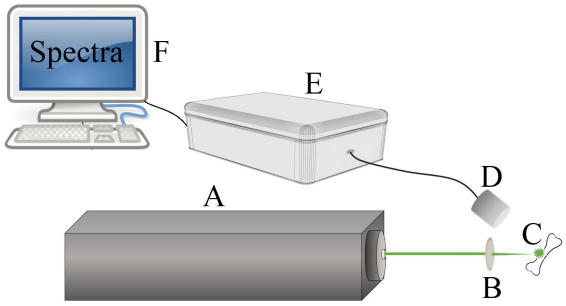

Fig. 1. The schematics of the LIBS setup. A: Laser (frequency-doubled Nd:YAG), B: Focusing lens, C: Generated plasma at the surface of the bone, D: Optical fiber and light collector, E: Echelle spectrometer, F: Computer.

E. Data Analysis

A total of 50 shots from the fresh sample and 50 shots from the dehydrated sample were taken, resulting in 100 spectra. After finding common peaks in both groups of samples which were in good agreement with those represented in the literature, 10 reproducible peaks among the whole spectra were chosen. Later on, 45 different ratios (all possible combinations) between the 10 chosen peak intensities were generated, using permutation without repetition. Canonical discriminant function analysis, as a well-known method in LIBS data processing [16, 24-26], was applied to these 45 peak intensity ratios to discriminate the fresh from the dehydrated bone. Lastly, the accuracy of the applied classifier was measured using a covariance matrix in both separate-groups and within-groups modes. In the within-groups mode, one-fold cross-validation was applied where each spectrum is classified by the function derived from the remaining ones.

III. Results

A. Original Grouped Cases

The observed atomic lines in the bone samples through LIBS were identified as calcium (Ca), sodium (Na), potassium (K), hydrogen (H), nitrogen (N), iron (Fe), and zinc (Zn). The observed atomic lines were in agreement with those described in the literature [9-18]. Figure 2 shows the classification result of the original grouped cases, dehydrated (dry) bone as group type 1 (upper histogram), and fresh bone as group type 2 (lower histogram). As is clear from the histograms shown in Fig. 2, the distribution of the dehydrated bone measurements (type 1) has a mean value of 2.77 (with a standard deviation of 1.035) while the fresh bone cases have the mean value of -2.77 (with a standard deviation of 0.964).

By employing the covariance matrix in separate-groups mode (original grouped cases), all of the 50 dehydrated cases were classified correctly as dehydrated bone (100 % accuracy), and 49 out of the 50 fresh cases as a fresh bone (98 % accuracy). Therefore, by employing the generated canonical discriminant function, in total 99 % of original grouped cases were classified correctly.

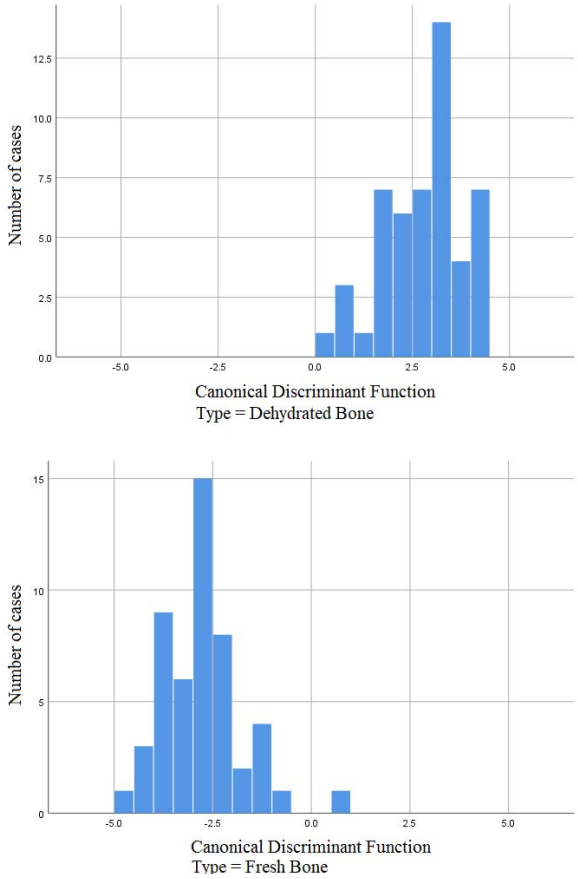

Fig. 2. Histogram graph of the group samples, dehydrated bone (upper), and fresh bone (lower). Unstandardized canonical discriminant functions evaluated at group centroid are +2.768 and -2.768 for dehydrated and fresh bone samples, respectively.

B. *Cross-Validated Grouped Cases*

In addition to the original grouped cases method, the validation method has been applied to make sure that the classifier is not overtrained. In the cross-validated mode, each case is classified by the function derived from the remaining cases. In within-groups mode (cross-validated grouped cases), 86 % of dehydrated cases, i.e. 43 out of 50, and 92 % of fresh cases, i.e. 46 out of 50, (89 % on average) were classified correctly. Since the accuracy in validation mode is also high, the classifier does not appear to be overtrained. Table 1 shows the predicted group membership in both original grouped cases and cross-validated grouped cases.

TABLE I. PREDICTED GROUP MEMBERSHIP

		Predicated Group Membership		
		Count (Percentage)		
		Dehydrated	Fresh	Total
Original	Dehydrated	50 (100 %)	0 (0 %)	50 (100 %)
	Fresh	1 (2 %)	49 (98 %)	50 (100 %)
Cross-validated	Dehydrated	43 (86 %)	7 (14 %)	50 (100 %)
	Fresh	4 (8 %)	46 (92%)	50 (100 %)

C. *ROC Analysis*

In addition, Receiver Operating Characteristic (ROC) analysis was also performed to confirm the performance of the proposed classifier. Figure 3. shows the result of the ROC analysis of the classifier. Sensitivity is shown in the vertical axis, and fall-out (1-specificity) on the horizontal axis. As it is clear from the figure, most of the area under the curve (AUC) is filled (more than 99 %), which is an indicator for the performance of the employed classifier to differentiate dehydrated from fresh bone.

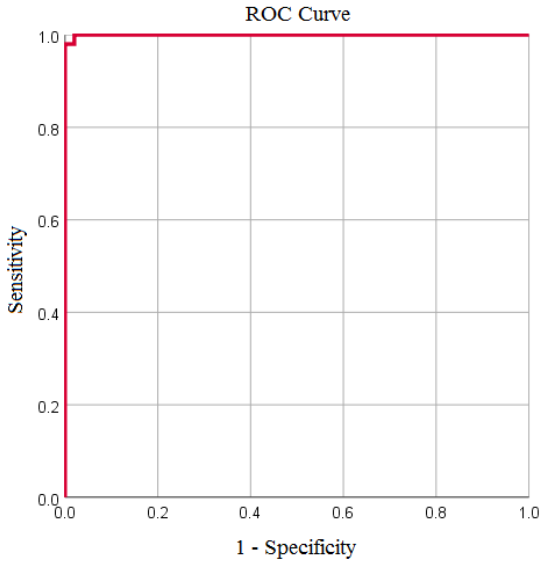

Fig. 3. ROC curve of the employed classifier. The area under the curve is more than 99 %.

IV. DISCUSSIONS

The preliminary results of this study confirmed the idea of bone dehydration detection through LIBS with an accuracy of 89 % in cross-validation mode. Regarding the high accuracy of validation, the classifier does not seem to be overfitting, even though only 45 ratios between intensities of 10 selected peaks were used as an input of the classifier. This pilot study was done with the assumption that the laser-induced dehydration process is similar to self-dehydration over time. Also, we applied the assumption that freezing keeps the original bone structure intact like in fresh bone. Further studies should be carried out to confirm these assumptions and also with a higher number of samples, before transferring the proposed method to the laserosteotomy system.

V. CONCLUSIONS

In conclusion, LIBS showed its potential to detect dehydration in bone with good accuracy in an *ex vivo* set-up. Although this pilot study was done with self-dehydration as compared to laser-induced dehydration, the results pave the way to the future work on real-time detection of laser-induced dehydration. Moreover, it should be mentioned that the future work needs to be performed with higher number of samples, to be able to add this feedback mechanism to laserosteotomes. In an experiment with a bigger number of samples, adding more inputs (peak intensities or ratios) to the classifier, the less likely the classifier will overfit, which could help to build a more robust discriminant function.

Also, a significant improvement for the further studies would be the ability to detect gradation in the degree of dehydration, instead of a yes/no decision.

REFERENCES

[1] Q. T. Le, R. Vilar, and C. Bertrand. "Influence of external cooling on the femtosecond laser ablation of dentin," Lasers Med. Sci., vol. 32, pp. 1943-1951, 2017.

[2] L. T. Cangueiro, and R. Vilar. "Influence of the pulse frequency and water cooling on the femtosecond laser ablation of bovine cortical bone," Appl. Surf. Sci., vol. 283, pp. 1012-1017, 2013.

[3] L. Kuscer, and J. Diaci, "Measurements of erbium laser-ablation efficiency in hard dental tissues under different water cooling conditions," J. Biomed. Opt., vol. 18, p. 108002, 2013.

[4] M. Augello, W. Deibel, K. Nuss, P. Cattin, P. and P. Jürgens, "Comparative microstructural analysis of bone osteotomies after cutting by computer-assisted robot-guided laser osteotome and piezoelectric osteotome: an in vivo animal study," Lasers Med. Sci., vol. 33, pp. 1-8, 2018.

[5] K-W. Baek, W. Deibel, D. Marinov, M. Griessen, A. Bruno, et al., "Clinical applicability of robot-guided contact-free laser osteotomy in cranio-maxillo-facial surgery: in-vitro simulation and in-vivo surgery in minipig mandibles," Br. J. Oral Maxillofac. Surg., vol. 53, pp. 976-981, 2015.

[6] D. G. Panduric, I. B. Juric, S. Music, K. Molcanov, M. Susic, et al., "Morphological and ultrastructural comparative analysis of bone tissue after Er: YAG laser and surgical drill osteotomy," Photomed. Laser Surg., vol. 32, pp. 401-408, 2014.

[7] H. Abbasi, L. Beltrán, G. Rauter, R. Guzman, P. C. Cattin, et al., "Effect of cooling water on ablation in Er: YAG laserosteotome of hard bone," Proc. SPIE., vol. 10453, 2017.

[8] L. M. B. Bernal, G. Shayeganrad, G. Kosa, M. Zelechowski, G. Rauter, et al., "Performance of Er: YAG laser ablation of hard bone under different irrigation water cooling conditions," Proc. SPIE, vol. 10492, 2018.

[9] R. Kanawade, F. Mahari, F. Klämpfl, M. Rohde, C. Knipfer, et al., "Qualitative tissue differentiation by analysing the intensity ratios of atomic emission lines using laser induced breakdown spectroscopy (LIBS): prospects for a feedback mechanism for surgical laser systems," J. Biophotonics, vol. 8. pp. 153-161, 2015.

[10] M. Rohde, F. Mehari, F. Klämpfl, W. Adler, F-W. Neukam, et al., "The differentiation of oral soft‐and hard tissues using laser induced breakdown spectroscopy‐a prospect for tissue specific laser surgery," J. Biophotonics, vol. 10, pp. 1250-1261, 2017.

[11] H. Abbasi, G. Rauter, R. Guzman, P. C. Cattin, and A. Zam, "Differentiation of femur bone from surrounding soft tissue using laser induced breakdown spectroscopy as a feedback system for smart laserosteotomy," Proc. SPIE, vol. 10685, 2018.

[12] M. Youngmin, J. H. Han, S. Shin, Y.-C. Kim, and S. Jeong, "Elemental analysis of tissue pellets for the differentiation of epidermal lesion and normal skin by laser-induced breakdown spectroscopy," Biomed. Opt. Express, vol. 7, pp. 1626-1636, 2016.

[13] F. Ghasemi, P. Parvin, N. S. H. Motlagh, A. Amjadi, and S. Abachi, "Laser induced breakdown spectroscopy and acoustic response techniques to discriminate healthy and cancerous breast tissues," Appl. Optics, vol. 55, pp. 8227-8235, 2016.

[14] B. Busser, S, Moncayo, J.-L. Coll, L. Sancey, and V. Motto-Ros, "Elemental imaging using laser-induced breakdown spectroscopy: A new and promising approach for biological and medical applications," Coord. Chem. Rev., vol. 358, pp. 70-79, 2018.

[15] S. A. Davari, S. Masjedi, Z. Ferdous, and D. Mukherjee, "In‐vitro analysis of early calcification in aortic valvular interstitial cells using Laser‐Induced Breakdown Spectroscopy (LIBS)," J. Biophotonics, vol. 11, p. e201600288, 2018.

[16] M. Bahreini, B. Ashrafkhani, and S. H. Tavassoli, "Discrimination of patients with diabetes mellitus and healthy subjects based on laser-induced breakdown spectroscopy of their fingernails," J. Biomed. Opt., vol. 18, p. 107006, 2013.

[17] R. K. Gill, F. Knorr, Z. J. Smith, M. Kahraman, D. Madsen, et al., "Characterization of femtosecond laser-induced breakdown spectroscopy (fsLIBS) and applications for biological samples," Appl. Spectrosc., vol. 68, pp. 949-954, 2014.

[18] R. K. Gill, Z. J. Smith, R. R. Panchal, J. W. Bishop, R. Gandour-Edwards, et al., "Preliminary fsLIBS study on bone tumors," Biomed. Opt. Express, vol. 6, pp. 4850-4858, 2015.

[19] Y. Moon, J. H. Han, J.-h. Choi, S. Shin, Y.-C. Kim, et al., "Mapping of cutaneous melanoma by femtosecond laser-induced breakdown spectroscopy," J. Biomed. Opt., vol. 24, p. 031011, 2018.

[20] X. Li, S. Yang, R. Fan, X. Yu, and D. Chen, "Discrimination of soft tissues using laser-induced breakdown spectroscopy in combination with k nearest neighbors (kNN) and support vector machine (SVM) classifiers," Opt. Laser Technol., vol. 120, pp. 233–239, 2018.

[21] H. Abbasi, G. Rauter, R. Guzman, P. C. Cattin, and A. Zam, "Laser-induced breakdown spectroscopy as a potential tool for autocarbonization detection in laserosteotomy," J. Biomed. Opt., vol. 23, p. 071206, 2018.

[22] H. Abbasi, G. Rauter, R. Guzman, P. C. Cattin, and A. Zam, "Plasma plume expansion dynamics in nanosecond Nd: YAG laserosteotome," Proc. SPIE, vol. 10505, 2018.

[23] M. Nazeri, A. E. Majd, R. Massudi, S. H. Tavassoli, A. Mesbahinia, et al., "Laser-induced breakdown spectroscopy via the spatially resolved technique using non-gated detector," J. Russ. Laser Res., vol. 37, pp. 164-171, 2016.

[24] C. Cocozzelli, "Understanding canonical discriminant function analysis: Testing typological hypotheses," J. Soc. Serv. Res., vol. 11, pp.93-117, 1988.

[25] Z. Hosseinimakarem, and S. H. Tavassoli, "Analysis of human nails by laser-induced breakdown spectroscopy," J. Biomed. Opt., vol. 16, p.057002, 2011.

[26] M. Bahreini, B. Ashrafkhani, S. H. and Tavassoli, "Elemental analysis of fingernail of alcoholic and doping subjects by laser-induced breakdown spectroscopy," Appl. Phys. B, vol. 114, pp.439-447, 2014.